Title

Linear weakening of the AMOC in response to receding glacial ice sheets in CCSM3

Journal

Geophysical Research Letters, 41(17)

ISSN

0094-8276

Authors

Zhu, Jiang
Liu, Zhengyu
Zhang, Xu
et al.

Publication Date

2014-09-16

DOI

10.1002/2014gl060891

Peer reviewed

AGU PUBLICATIONS

Geophysical Research Letters

RESEARCH LETTER
10.1002/2014GL060891

Key Points:
- The AMOC weakens greatly in response to deglacial lowering ice sheet topography
- This weakening follows a strikingly linear relationship with ice sheet volume
- The weakening is caused by a wind-driven sea ice expansion process

Supporting Information:
- Readme
- Figures S1–S4
- Text S1–S4

Correspondence to:
J. Zhu and Z. Liu,
jzhu47@wisc.edu;
zliu3@wisc.edu

Citation:
Zhu, J., Z. Liu, X. Zhang, I. Eisenman, and W. Liu (2014), Linear weakening of the AMOC in response to receding glacial ice sheets in CCSM3, *Geophys. Res. Lett.*, *41*, 6252–6258, doi:10.1002/2014GL060891.

Received 17 JUN 2014
Accepted 14 AUG 2014
Accepted article online 19 AUG 2014
Published online 3 SEP 2014

Linear weakening of the AMOC in response to receding glacial ice sheets in CCSM3

Jiang Zhu[1], Zhengyu Liu[1,2], Xu Zhang[3], Ian Eisenman[4], and Wei Liu[4]

[1]Department of Atmospheric and Oceanic Sciences and Center for Climatic Research, University of Wisconsin-Madison, Madison, Wisconsin, USA, [2]Laboratory for Climate and Ocean-Atmosphere Studies, School of Physics, Peking University, Beijing, China, [3]Alfred Wegener Institute Helmholtz Centre for Polar and Marine Research, Bremerhaven, Germany, [4]Scripps Institution of Oceanography, University of California, San Diego, La Jolla, California, USA

Abstract The transient response of the Atlantic Meridional Overturning Circulation (AMOC) to a deglacial ice sheet retreat is studied using the Community Climate System Model version 3 (CCSM3), with a focus on orographic effects rather than meltwater discharge. It is found that the AMOC weakens significantly (41%) in response to the deglacial ice sheet retreat. The AMOC weakening follows the decrease of the Northern Hemisphere ice sheet volume linearly, with no evidence of abrupt thresholds. A wind-driven mechanism is proposed to explain the weakening of the AMOC: lowering the Northern Hemisphere ice sheets induces a northward shift of the westerlies, which causes a rapid eastward sea ice transport and expanded sea ice cover over the subpolar North Atlantic; this expanded sea ice insulates the ocean from heat loss and leads to suppressed deep convection and a weakened AMOC. A sea ice-ocean positive feedback could be further established between the AMOC decrease and sea ice expansion.

1. Introduction

Ice sheets actively influence the climate system because of their orographic features, their albedo, and their function as the largest readily exchangeable reservoir of fresh water on Earth [e.g., *Clark et al.*, 1999]. Paleoclimate records have shown that global ice sheet volume during the late Quaternary has varied significantly with the glacial-interglacial cycles, possibly driven by variations in Earth's orbit [*Hays et al.*, 1976; *Shackleton*, 2000]. Along with the waxing and waning of ice sheets, the Atlantic Meridional Overturning Circulation (AMOC) is also thought to have experienced significant changes [*McManus et al.*, 2004; *Rahmstorf*, 2002], with a possible contribution to the abrupt climate changes in the North Atlantic region and the globe [*Clark et al.*, 2002].

Previous studies regarding the influence of ice sheet retreat on the AMOC have focused on the effects of meltwater discharge [*Broecker*, 1994; *Hu et al.*, 2009, and references therein], while the role of the associated reorganization of atmospheric circulation induced by the changing orography has been largely neglected. Recently, a modeling study [*Eisenman et al.*, 2009] suggested that anomalous rainfall over the northern North Atlantic Ocean associated with orographic forcing from the receding glacial ice sheets could cause a decrease in the AMOC and a possible abrupt climate change. However, other studies that also used coupled climate models postulated different mechanisms for the weakening of the AMOC, e.g., the adjustment of sea ice coverage [*Vettoretti and Peltier*, 2013; *Zhang et al.*, 2014] and variations in wind-driven ocean circulations [*Zhang et al.*, 2014] caused by ice sheet changes. Therefore, basic questions remain regarding the AMOC response to the orographic effects of receding ice sheets, and the underlying mechanisms are still open to debate. Furthermore, in studies only using fully coupled models the mechanism driving a response typically remains ambiguous due to the complicated feedbacks involved and the coupled nature of the climate system, and companion simulations in which some components of the climate system are inactivated help elucidate physical mechanisms [*Eisenman et al.*, 2009].

Another question of great interests related to the ice sheet retreat is whether a gradual variation in the ice sheet volume could trigger abrupt shifts in the AMOC [*Wunsch*, 2006] through factors such as freshwater forcing [*Rahmstorf*, 1995] or heat flux forcing [*Oka et al.*, 2012]. *Zhang et al.* [2014] has recently demonstrated that, in their coupled general circulation model, variations in intermediate ice sheet volume could cause abrupt changes in the AMOC and rapid glacial climate shifts via the northern westerly shifts associated with the ice sheet orographic changes. Given the model uncertainty on simulating glacial ocean

circulation [*Otto-Bliesner et al.*, 2007], this nonlinear behavior of the AMOC should be carefully examined across multiple climate models.

The objective of this paper is to study the transient response of the AMOC to a realistic deglacial lowering of ice sheets in the Community Climate System Model version 3 (CCSM3) and further investigate the underlying mechanisms by using both atmosphere-alone and fully coupled simulations. Our study suggests that the retreat of the Northern Hemisphere ice sheets induces a northward shift of the westerlies in the northern North Atlantic. This shift causes a rapid sea ice expansion and enhanced insulation against oceanic heat loss to the atmosphere, which then leads to a reduction of deep convection and eventually a weaker AMOC. The transient weakening of the AMOC is gradual in CCSM3 with respect to the ice sheet topographic forcing, with no evidence of nonlinear thresholds. The remainder of this paper is arranged as follows: Section 2 briefly describes the model and experiments. The evolution of the AMOC to a realistic deglacial lowering of ice sheets is shown in section 3. We then investigate the underlying mechanisms in section 4. A summary and further discussion is given in section 5.

2. Model and Experiments

We analyze a transient simulation of climate evolution over the last 21,000 years forced only by the receding ice sheets (TraIS, hereafter) in a low-resolution version of CCSM3 [*Yeager et al.*, 2006]. The model components include the Community Atmosphere Model 3 (CAM3) at T31 horizontal resolution with 26 vertical levels, the Community Land Model 3 also at T31 resolution, the Parallel Ocean Program at a nominal 3° horizontal resolution with 25 vertical levels, and the Community Sea Ice Model 5 on the same horizontal grid as the ocean. TraIS is branched off from a transient simulation of the last 21,000 years [*Z. Liu et al.*, 2009] at 19 ka before present (A.D. 1950) and is integrated to the present day [*He et al.*, 2013; *Shakun et al.*, 2012]. The ice sheet configuration in the simulation is altered every 500 years based on the ICE-5G reconstruction [*Peltier*, 2004]; the solar insolation, greenhouse gases (GHGs), and ocean bathymetry are prescribed at the value of 19 ka, and the effect of freshwater flux associated with the ice sheet melting is not included.

In addition to the transient simulation with the fully coupled CCSM3, two atmosphere-only simulations using the same atmosphere component model (CAM3) are employed in this study (LARGEatm and MEDIUMatm [*Eisenman et al.*, 2009]). The sea surface temperature and sea ice cover in both simulations are specified to follow the seasonal cycle from a coupled simulation at 21 ka. The two runs only differ in the ice sheet configuration and GHG concentrations: LARGEatm uses the ice sheets and GHGs at 21 ka while MEDIUMatm makes use of those at 12 ka. Readers are referred to *Eisenman et al.* [2009] for the details of these two experiments. The difference in an atmospheric variable between MEDIUMatm and LARGEatm mainly represents its response to receding ice sheets excluding the possible feedbacks from other components involving sea ice and ocean (the contribution from difference GHG concentrations is expected to be small since both runs use the same prescribed sea surface temperature and sea ice) [*Eisenman et al.*, 2009].

3. Linear Weakening of the AMOC to Receding Ice Sheets

In the transient ice sheet simulation, the maximum AMOC decreases following the lowering of the Northern Hemisphere ice sheets, as shown in Figure 1. At 19 ka, the AMOC maximum is 11.5 sverdrup (Sv), comparable to that at the Last Glacial Maximum (LGM, 22–19 ka) in the transient simulation with all climatic forcing, including GHGs, insolation, ice sheets, and freshwater fluxes [*Z. Liu et al.*, 2009]. In response to the deglacial receding of ice sheets, the AMOC weakens by 41%, a significant amount compared with glacial variations and changes that result from other climatic factors as suggested by paleoclimate reconstructions [*McManus et al.*, 2004] and numerical simulations [*He et al.*, 2013; *Z. Liu et al.*, 2009; *Shakun et al.*, 2012; *Zhu et al.*, 2014]. These results imply that the orographic effects alone associated with glacial variations in ice sheets can cause significant changes in the AMOC and, in turn, the climate at regional and global scales (Figure S1 and Text S1 in the supporting information).

Notably, the AMOC strength and the Northern Hemisphere ice sheet volume exhibit a strikingly linear relationship with a correlation coefficient larger than 0.9 (Figure 1b). The linear regression coefficient (with a 95% confidence interval) is 4.7 ± 0.2 Sv per total deglacial change of ice sheets. Although the temporal evolution of the AMOC strength shows an abrupt reduction at 14 ka, it is accompanied by the

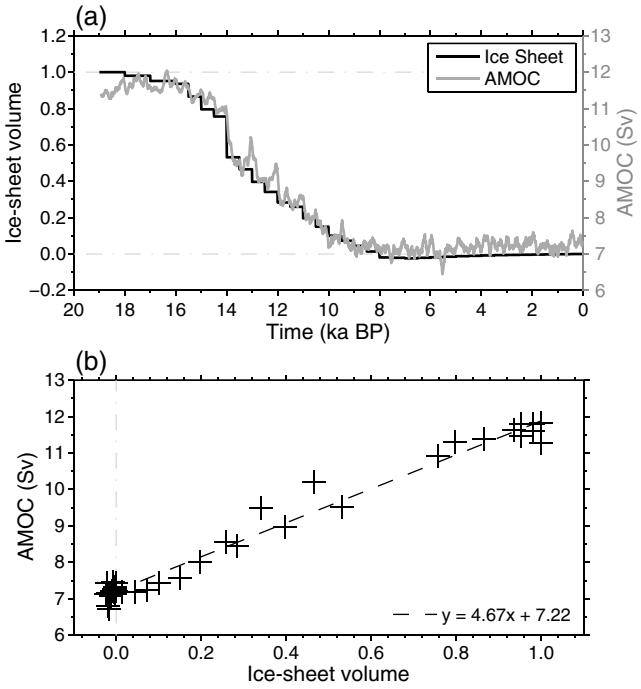

Figure 1. (a) Time series of the Northern Hemisphere ice sheet volume (black, left axis) and the maximum AMOC in the transient simulation (gray, right axis, units: Sv = 10^6 m^3 s^{-1}). (b) Scatterplot of the maximum AMOC and the Northern Hemisphere ice sheet volume. Note that the ice sheet height/volume is altered every 500 years in the transient simulation, the time series of the AMOC is from the decadal mean data, and the mean values of the maximum AMOC over the last 100 years within each interval are used to produce the scatterplot in Figure 1b. For illustration purpose, the ice sheet volume has been rescaled between 0 and 1.

largest retreat of ice sheets (22% by volume, corresponding roughly to meltwater pulse 1A). Therefore, their linear relationship is still evident. Our CCSM3 simulation results do not support the possibility that the ice sheet orographic forcing is able to trigger a nonlinear "switch-like" response in the AMOC, at odds with *Zhang et al.* [2014].

4. Changes in Low-Level Winds and Sea Ice Transport

To understand the dynamic mechanisms of the AMOC response to receding ice sheets, we examine the changes in low-level winds in both the atmosphere-only simulations and fully coupled transient simulation. At the LGM (19–18 ka in TraIS), the model simulates a westerly jet across the Atlantic that is nearly zonal along ~40°N, with cyclonic and anticyclonic winds to the north and south, respectively (Figure 2a). In response to ice sheet retreat, the atmosphere-only simulations (MEDIUMatm − LARGEatm) reveal anticyclonic wind changes over the North Atlantic with changes in magnitude up to 5 m s^{-1} (Figure 2b), which is a manifestation of the northward shift of the westerly jet [*Kutzbach and Guetter*, 1986; *Manabe and Broccoli*, 1985]. Comparable anticyclonic wind changes also stand out in TraIS at 12 ka (Figure 2c), suggesting the same origin for the atmospheric response to ice sheets as the orographic effects [*Pausata et al.*, 2011]. The pattern of wind response at 850 hPa is robust across the entire transient simulation (see also Figure 4b) and is coherent with the surface wind stress (Figure 3b). It is worth noting that, in

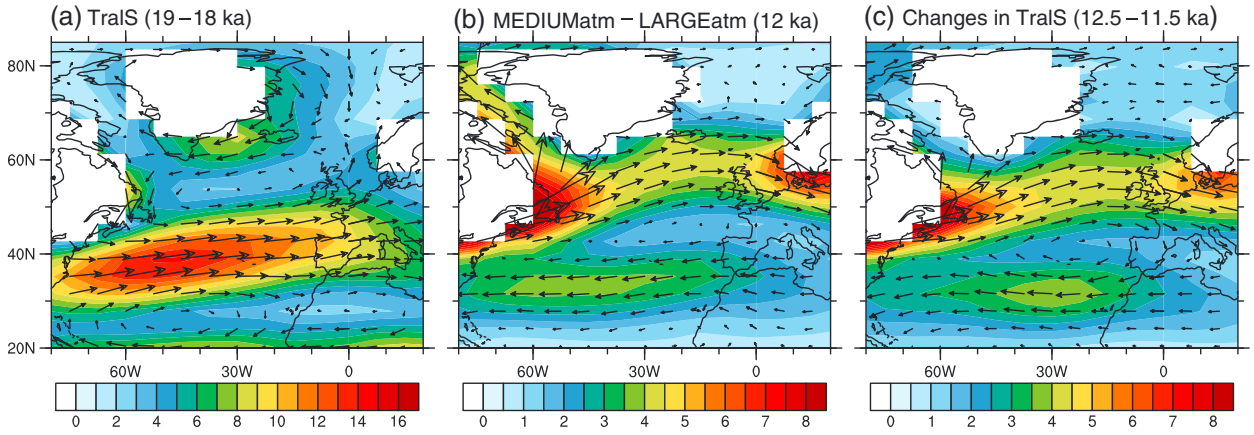

Figure 2. (a) Climatological annual mean winds at 850 hPa (vectors, units: m s^{-1}) over the North Atlantic before the lowering of ice sheets (averaged between 19 and 18 ka). (b) Differences in the annual mean winds at 850 hPa in the atmosphere-alone simulations with the ice sheet volume at 12 and 21 ka respectively. (c) The same as Figure 2b, but for the fully coupled transient simulation. Shading denotes the magnitude of the wind vectors.

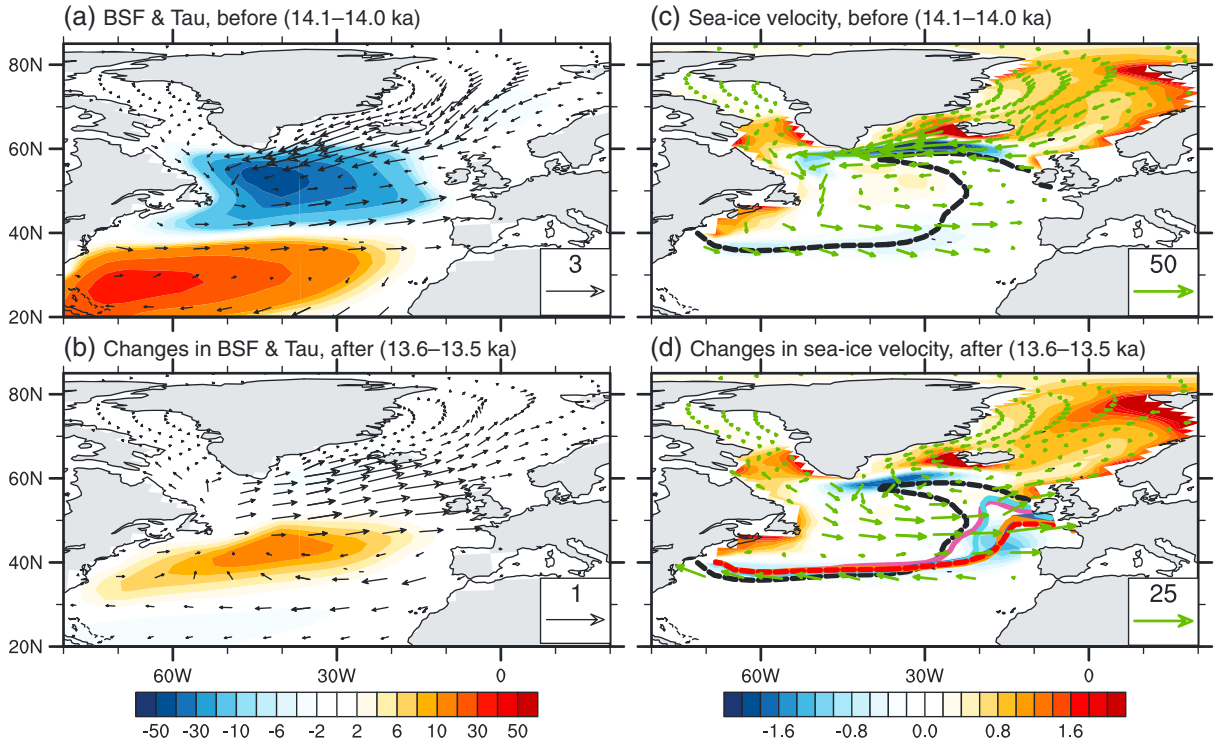

Figure 3. (a) Last 100 year (14.1–14.0 ka) average before the 14 ka transition of the annual mean barotropic stream function (BSF, shading, units: Sv) and surface wind stress (black vectors, units: dyn cm^{-2}). (b) 401–500 years (13.6–13.5 ka) average after the 14 ka transition of the changes in barotropic stream function and surface wind stress. (c) Last 100 year (14.1–14.0 ka) average before the 14 ka transition of the annual mean sea ice formation rate (shading, units: cm d^{-1}), sea ice velocity (green vectors, units: cm s^{-1}), and the February sea ice margin (defined as the 15% sea ice coverage) (black dashed). (d) 401–500 years (13.6–13.5 ka) average after the 14 ka transition of the sea ice formation rate, changes in sea ice velocity, and the progression of the February sea ice margin (black dashed, before the transition; magenta, the first year; blue, years 5–15; cyan, years 45–55; dark orange, years 95–105; red dashed, years 401–500).

response to receding ice sheets, TraIS is characterized by a marked cooling in the northern high latitudes, especially over ocean in the Labrador Sea and the Greenland, Iceland, and Norwegian Seas, as well as a weaker warming in the Southern Hemisphere (Figure S1), indicating important feedbacks from ocean and sea ice adjustments.

The anomalous westerly winds in the Atlantic midlatitudes can cause a significant expansion of sea ice through wind-driven processes, as explained below. The abrupt transition at 14 ka provides an example. Before the transition, the wind-driven counterclockwise subpolar gyre and clockwise subtropical gyre are distinct in the ocean (Figure 3a). Sea ice generally forms in the northern and western parts of the subpolar region (Figure 3c, shading with warm color), moves southward and eastward (green vectors) due to wind-driven processes (Figure 3a), and melts to the south of Greenland (~60°N) and the midlatitudes (~40°N) (Figure 3c, shading with cold color), producing an "s-shaped" February sea ice margin (black dashed contour). After the sudden lowering of ice sheets, there is an evident northward shift of the gyre systems: a strengthening of the subtropical gyre along its northern edge and a weakening of the subpolar gyre along its southern edge (40°N–50°N) (Figure 3b). Consequently, sea ice is transported anomalously eastward in the northern part (~50°N) and westward in the southern part (~40°N) (Figure 3d, green vectors), causing rapid reorganization of the sea ice into a more zonal shape (contours). The blue, magenta, cyan, dark orange, and dashed red contours represent the February sea ice margin for the year 1, years 5–15, years 45–55, years 95–105, and years 401–500 average after the transition, respectively. The most striking feature is that a significant part of the sea ice expansion can be accomplished within 1 year. This rapid sea ice expansion implies the key role of the varied wind stress on sea ice transport, because the local sea ice formation (shading) is insignificant. Specifically, it is found that the change in the thermodynamic sea ice volume tendency over the northern North Atlantic is negative and smaller than the positive value in the dynamic volume tendency (Figure S2 and Text S2), supporting the interpretation that sea ice transport is the primary

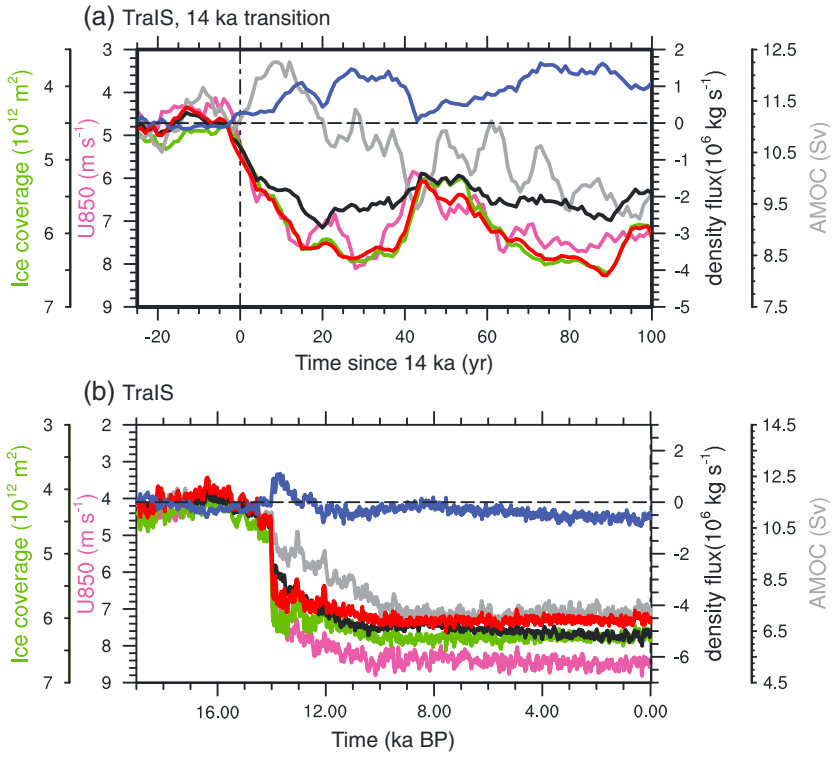

Figure 4. (a) Time series of the annual mean area-averaged zonal wind at 850 hPa (magenta, first left axis), sea ice area (green, second left axis), area-integrated total, thermal, and haline surface density flux (black, red, and blue, respectively, first right axis) and the maximum AMOC (gray, second right axis) over the northern North Atlantic (50–70°N) near the 14 ka transition. (b) As in Figure 4a, but for the time series of decadal means in the entire transient simulation.

factor contributing to the expansion. Note that this rapid response in sea ice cover could not have resulted from the weakening of the AMOC, because the timescales of the latter is much longer than several years.

The wind-induced sea ice expansion, especially over the deep water formation region, can inhibit the deep convection and eventually weaken the AMOC through the sea ice insulating effect (Figure S3 and Text S3). Afterward, the weakened AMOC can further enhance the sea ice expansion through the reduced northward heat transport (Figure S4 and Text S4), forming a positive feedback between the sea ice expansion and the AMOC weakening [*Jayne and Marotzke*, 1999; *Zhong et al.*, 2011]. We note that changes in sea surface density from anomalous precipitation and evaporation (including river runoff, Figures S3g and S3h) are relatively small and therefore do not appear to play a dominant role in changing the AMOC. This is in contrast to the rain-driven mechanism proposed by *Eisenman et al.* [2009], and possible explanations are a topic for further study.

Our proposed mechanism involving wind-induced sea ice expansion and the subsequent insulating effect can be further supported by analyzing the evolution of the zonal wind, sea ice coverage, and surface buoyancy fluxes over the North Atlantic subpolar region (50–70°N). In TraIS, after the sudden ice sheet lowering at 14 ka (Figure 4a), both the zonal wind and sea ice cover exhibit a rapid adjustment in the first few years, with an increase of 62% in wind (from 4.5 to 7.3 m s^{-1}, magenta, first left axis) and 32% in sea ice cover (from 4.7 to 6.2×10^{12} m^2, green, second left axis). Simultaneously, the area-integrated thermal density flux (heat flux-induced density changes) decreases by 49% (red, first right axis), reducing the total density flux substantially (black, first right axis). In comparison, the AMOC does not decrease dramatically until almost 20 years after the sudden ice sheet lowering. Therefore, the initial expansion of sea ice does not appear to be caused by the weakening of the AMOC. We further hypothesize that the wind-driven sea ice expansion mechanism seems to be critical not only for the 14 ka transition but also for the entire deglaciation period in the transient weakening of the AMOC (Figure 4b). The evolution of the zonal wind at 850 hPa, the expansion of sea ice, and the reduction of surface density fluxes are all coherent with the weakening of the AMOC.

5. Summary and Discussion

The evolution of the AMOC in response to a deglacial lowering of ice sheets is studied using a transient simulation in the CCSM3. Focus is placed on the effects of ice sheet orography, rather than the associated deglacial meltwater discharge. The simulation indicates that, as the Northern Hemisphere ice sheets recede, the AMOC weakens significantly. Furthermore, the AMOC weakening appears to be gradual during the entire deglaciation simulation, exhibiting an approximately linear response to the Northern Hemisphere ice sheet volume with no clear nonlinear thresholds. A wind-driven mechanism is proposed to explain this weakening: lowering of ice sheets induces a northward shift of the westerlies and a rapid eastward sea ice transport and expansion in the northern North Atlantic, which insulates the ocean from heat loss and eventually leads to suppressed deep convection and weakened AMOC. This AMOC reduction could be further sustained by a positive feedback between the sea ice expansion and the reduction of the northward heat transport by the AMOC at decadal and longer timescales. Our findings reveal that the response of wind fields, and in turn the induced sea ice transport, plays a key role in the reduction of the AMOC in response to the orographic effects of ice sheet retreat [cf. *Vettoretti and Peltier*, 2013; *Zhang et al.*, 2014].

Our experiment suggests a linear weakening of the AMOC, in contrast to the nonlinear behavior described in *Zhang et al.* [2014]. This difference could be related to the different AMOC stability and initial background climates in the two models. In CCSM3, the AMOC is in a stable regime with a single equilibrium under the present day and the LGM climates [*W. Liu et al.*, 2013, 2014a], and even during the last deglaciation [*W. Liu et al.*, 2014b]. However, in *Zhang et al.* [2014], they reported that their model (COSMOS, ECHAM5-JSBACH-MPIOM) is in a bistable regime with a strong and a weak AMOC mode coexisting. Furthermore, in comparison to the corresponding preindustrial control simulation, the LGM ocean circulation in CCSM3 is characterized by a shallower and weaker AMOC, while a slightly stronger and shallower AMOC is found in COSMOS [*Zhang et al.*, 2013]. These discrepancies call for more modeling research on the AMOC dynamics and its response to the orographic effects of receding ice sheets in coupled models.

Findings in this study imply that in order to understand the role of ice sheets in glacial-interglacial climate change, we need to explicitly consider both the orographic effects and the traditional melting water discharge [cf. *Eisenman et al.*, 2009; *Zhang et al.*, 2014]. Furthermore, our experiments do not support the possibility that the ice sheet orographic forcing is able to trigger a nonlinear switch-like response in the AMOC. Nevertheless, they do demonstrate that a sufficiently fast lowering of the ice sheet topography alone (without meltwater discharge), like the 22% decrease by volume at 14 ka, can cause a large and rapid response in the thermohaline circulation and, therefore, regional and global abrupt climate change, through wind field changes [*Wunsch*, 2006]. Notably, in simulations incorporating the deglacial GHG forcing, the decreased AMOC in our study could be greatly overcompensated, as the AMOC at the LGM is suggested to increase more significantly in response to the sole forcing of deglacial GHGs [*Shakun et al.*, 2012; *Zhu et al.*, 2014], resulting in a stronger modeled AMOC at the present day.

It should be noted that the proposed mechanism involving sea ice expansion could depend on the background climate state. In a warmer climate with relative small sea ice coverage in the northern North Atlantic, other factors such as the anomalous precipitation and gyre salt transport [*Born et al.*, 2010; *Schiller et al.*, 1997; *Timmermann and Goosse*, 2004] could play a major role. It is also interesting to find that there is an evident tendency for the AMOC to recover for some steps of ice sheet lowering (e.g., at 13.5 and 12.5 ka), but not for others (e.g., 14.0 and 13.0 ka). Additional experiments are needed to study the dependence of the AMOC response on the background climate and details of ice sheet forcing, but are beyond the scope of this study.

Acknowledgments

The authors thank Feng He for performing the transient experiments. This work is supported by NSF (grant ARC-1107795), NSFC 41130105, MOST 2012CB955200, and DOE. X.Z. is supported by the Helmholtz Graduate School for Polar and Marine Research (POLMAR) and Helmholtz funding through the Polar Regions and Coasts in the changing Earth System (PACES) programme of the Alfred Wegener Institute Helmholtz Centre for Polar and Marine Research. The output of the CCSM3 experiments can be obtained by sending a written request to the corresponding author.

The Editor thanks three anonymous reviewers for their assistance in evaluating this paper.

References

Born, A., K. Nisancioglu, and P. Braconnot (2010), Sea ice induced changes in ocean circulation during the Eemian, *Clim. Dyn.*, *35*(7-8), 1361–1371, doi:10.1007/s00382-009-0709-2.

Broecker, W. S. (1994), Massive iceberg discharges as triggers for global climate change, *Nature*, *372*(6505), 421–424, doi:10.1038/372421a0.

Clark, P. U., R. B. Alley, and D. Pollard (1999), Northern Hemisphere ice-sheet influences on global climate change, *Science*, *286*(5442), 1104–1111, doi:10.1126/science.286.5442.1104.

Clark, P. U., N. G. Pisias, T. F. Stocker, and A. J. Weaver (2002), The role of the thermohaline circulation in abrupt climate change, *Nature*, *415*(6874), 863–869, doi:10.1038/415863a.

Eisenman, I., C. M. Bitz, and E. Tziperman (2009), Rain driven by receding ice sheets as a cause of past climate change, *Paleoceanography*, *24*, PA4209, doi:10.1029/2009PA001778.

Hays, J. D., J. Imbrie, and N. J. Shackleton (1976), Variations in the Earth's orbit: Pacemaker of the ice ages, *Science*, *194*(4270), 1121–1132, doi:10.1126/science.194.4270.1121.

He, F., J. D. Shakun, P. U. Clark, A. E. Carlson, Z. Liu, B. L. Otto-Bliesner, and J. E. Kutzbach (2013), Northern Hemisphere forcing of Southern Hemisphere climate during the last deglaciation, *Nature*, *494*(7435), 81–85, doi:10.1038/nature11822.

Hu, A., G. A. Meehl, W. Han, and J. Yin (2009), Transient response of the MOC and climate to potential melting of the Greenland ice sheet in the 21st century, *Geophys. Res. Lett.*, *36*, L10707, doi:10.1029/2009GL037998.

Jayne, S. R., and J. Marotzke (1999), A destabilizing thermohaline circulation-atmosphere-sea ice feedback, *J. Clim.*, *12*(2), 642–651, doi:10.1175/1520-0442(1999)012<0642:adtcas>2.0.co;2.

Kutzbach, J. E., and P. J. Guetter (1986), The influence of changing orbital parameters and surface boundary conditions on climate simulations for the past 18 000 years, *J. Atmos. Sci.*, *43*(16), 1726–1759, doi:10.1175/1520-0469(1986)043<1726:tiocop>2.0.co;2.

Liu, W., Z. Liu, and A. Hu (2013), The stability of an evolving Atlantic meridional overturning circulation, *Geophys. Res. Lett.*, *40*, 1562–1568, doi:10.1002/grl.50365.

Liu, W., Z. Liu, and E. C. Brady (2014a), Why is the AMOC monostable in coupled general circulation models?, *J. Clim.*, *27*(6), 2427–2443, doi:10.1175/JCLI-D-13-00264.1.

Liu, W., Z. Liu, J. Cheng, and H. Hu (2014b), On the stability of the Atlantic meridional overturning circulation during the last deglaciation, *Clim. Dyn.*, doi:10.1007/s00382-014-2153-1, in press.

Liu, Z., et al. (2009), Transient simulation of last deglaciation with a new mechanism for Bølling-Allerød warming, *Science*, *325*(5938), 310–314, doi:10.1126/science.1171041.

Manabe, S., and A. J. Broccoli (1985), The influence of continental ice sheets on the climate of an ice age, *J. Geophys. Res.*, *90*(D1), 2167–2190, doi:10.1029/JD090iD01p02167.

McManus, J. F., R. Francois, J. M. Gherardi, L. D. Keigwin, and S. Brown-Leger (2004), Collapse and rapid resumption of Atlantic meridional circulation linked to deglacial climate changes, *Nature*, *428*(6985), 834–837, doi:10.1038/nature02494.

Oka, A., H. Hasumi, and A. Abe-Ouchi (2012), The thermal threshold of the Atlantic meridional overturning circulation and its control by wind stress forcing during glacial climate, *Geophys. Res. Lett.*, *39*, L09709, doi:10.1029/2012GL051421.

Otto-Bliesner, B. L., C. D. Hewitt, T. M. Marchitto, E. Brady, A. Abe-Ouchi, M. Crucifix, S. Murakami, and S. L. Weber (2007), Last Glacial Maximum ocean thermohaline circulation: PMIP2 model intercomparisons and data constraints, *Geophys. Res. Lett.*, *34*, L12706, doi:10.1029/2007GL029475.

Pausata, F. S. R., C. Li, J. J. Wettstein, M. Kageyama, and K. H. Nisancioglu (2011), The key role of topography in altering North Atlantic atmospheric circulation during the last glacial period, *Clim. Past*, *7*(4), 1089–1101, doi:10.5194/cp-7-1089-2011.

Peltier, W. R. (2004), Global glacial isostasy and the surface of the ice-age Earth: The ICE-5G (VM2) model and GRACE, *Annu. Rev. Earth Planet. Sci.*, *32*(1), 111–149, doi:10.1146/annurev.earth.32.082503.144359.

Rahmstorf, S. (1995), Bifurcations of the Atlantic thermohaline circulation in response to changes in the hydrological cycle, *Nature*, *378*(6553), 145–149, doi:10.1038/378145a0.

Rahmstorf, S. (2002), Ocean circulation and climate during the past 120,000 years, *Nature*, *419*(6903), 207–214, doi:10.1038/nature01090.

Schiller, A., U. Mikolajewicz, and R. Voss (1997), The stability of the North Atlantic thermohaline circulation in a coupled ocean-atmosphere general circulation model, *Clim. Dyn.*, *13*(5), 325–347, doi:10.1007/s003820050169.

Shackleton, N. J. (2000), The 100,000-year ice-age cycle identified and found to lag temperature, carbon dioxide, and orbital eccentricity, *Science*, *289*(5486), 1897–1902, doi:10.1126/science.289.5486.1897.

Shakun, J. D., P. U. Clark, F. He, S. A. Marcott, A. C. Mix, Z. Liu, B. Otto-Bliesner, A. Schmittner, and E. Bard (2012), Global warming preceded by increasing carbon dioxide concentrations during the last deglaciation, *Nature*, *484*(7392), 49–54, doi:10.1038/nature10915.

Timmermann, A., and H. Goosse (2004), Is the wind stress forcing essential for the meridional overturning circulation?, *Geophys. Res. Lett.*, *31*, L04303, doi:10.1029/2003GL018777.

Vettoretti, G., and W. R. Peltier (2013), Last Glacial Maximum ice sheet impacts on North Atlantic climate variability: The importance of the sea ice lid, *Geophys. Res. Lett.*, *40*, 6378–6383, doi:10.1002/2013GL058486.

Wunsch, C. (2006), Abrupt climate change: An alternative view, *Quatern. Res.*, *65*(2), 191–203, doi:10.1016/j.yqres.2005.10.006.

Yeager, S. G., C. A. Shields, W. G. Large, and J. J. Hack (2006), The low-resolution CCSM3, *J. Clim.*, *19*(11), 2545–2566, doi:10.1175/jcli3744.1.

Zhang, X., G. Lohmann, G. Knorr, and X. Xu (2013), Different ocean states and transient characteristics in Last Glacial Maximum simulations and implications for deglaciation, *Clim. Past*, *9*(5), 2319–2333, doi:10.5194/cp-9-2319-2013.

Zhang, X., G. Lohmann, G. Knorr, and C. Purcell (2014), Abrupt glacial climate shifts controlled by ice sheet changes, *Nature*, doi:10.1038/nature13592, in press.

Zhong, Y., G. H. Miller, B. L. Otto-Bliesner, M. M. Holland, D. A. Bailey, D. P. Schneider, and A. Geirsdottir (2011), Centennial-scale climate change from decadally-paced explosive volcanism: A coupled sea ice-ocean mechanism, *Clim. Dyn.*, *37*(11-12), 2373–2387, doi:10.1007/s003820-010-0967-z.

Zhu, J., Z. Liu, J. Zhang, and W. Liu (2014), AMOC response to global warming: Dependence on the background climate and response timescale, *Clim. Dyn.*, doi:10.1007/s00382-014-2165-x, in press.

Auxiliary material for

Linear Weakening of the AMOC in response to Receding Glacial Ice Sheets in CCSM3

Jiang Zhu[1] , Zhengyu Liu[1,2], Xu Zhang[3], Ian Eisenman[4], and Wei Liu[4]

[1]Department of Atmospheric and Oceanic Sciences and Center for Climatic Research, University of Wisconsin-Madison, Madison, Wisconsin 53706, USA

[2]Laboratory for Climate and Ocean-Atmosphere Studies, School of Physics, Peking University, Beijing 100871, China

[3]Alfred Wegener Institute for Polar and Marine Research, Bussestrasse 24, D-27570 Bremerhaven, Germany

[4]Scripps Institution of Oceanography, University of California, San Diego, La Jolla, California 92093, USA

Geophysical Research Letters

Introduction

These auxiliary material files contain supplemental figures and discussion that support the main text of the article.

Figures S1–S4.docx: Supplementary figures with captions included.

Text S1–S4.docx: Discussion on supplementary figures and references.

Figures S1–S4

Figure Captions

Figure S1. (a) Time series of the Northern Hemisphere ice-sheet volume (black, left axis) and the global (gray), North Atlantic (red, 80ºW–20ºE, 0–90ºN) and South Atlantic (blue, 60ºW–20ºE, 0–90ºS) annual mean surface temperature (TS) in the transient simulation (right axis). (b) Changes in TS calculated as the difference between after (13.6–13.5 ka) and before (14.1–14.0 ka) the 14 ka transition. (c) Changes in TS calculated as the difference between after (1.0–0 ka) and before (19.0–18.0 ka) the removal of glacial ice sheets. For illustration purpose, the ice-sheet volume in (a) has been rescaled between 0 and 1.

Figure S2. Budget of the anomalous area-integrated annual-mean sea-ice volume tendency over the subpolar Atlantic (50ºN–70ºN) after the 14 ka transition. The net sea-ice tendency and the separation between the dynamical formation and thermodynamical formation for the first 20 years (14.00–13.98 ka) and the last 100 years (13.6–13.5 ka) are shown, respectively. Anomalies are from the last 100 years before the 14 ka transition (14.1–14.0 ka) and integrated over the subpolar North Atlantic (45–65ºN), where deep convection takes place in the modeled LGM climate.

Figure S3. (a) Last 100 years average (14.1–14.0 ka) before the 14 ka transition of the annual mean density flux (shading, units: 10^{-6} kg m^{-2} s^{-1}; positive means flux makes water more dense), the March mixed layer depth (black contour, contour interval: 200 m), and the February sea-ice margin (green contour). (b) the same as (a), except for variables averaged over 401–500 years (13.6–13.5 ka) after the transition. (c) and (d) are the same as (a) and (b), but the shadings

are for the thermal component of the surface density flux. (e) and (f) are the same as (a) and (b), but the shadings are for the haline component of the surface density flux. (g) and (h) are the same as (a) and (b), but the shadings are for the density flux induced by P – E + R (i.e., not including contribution from sea-ice forming and melting).

Figure S4. (a) Evolution of the anomalous northward total (black), the meridional part (red) and the azonal part (blue) heat transport across 45ºN in the Atlantic Ocean near the 14 ka transition (units: PW = 10^{15} watts). (b) as in (a), but for freshwater transport (units: Sv = 10^6 m^3 s^{-1}).

Figures

Figure S1.

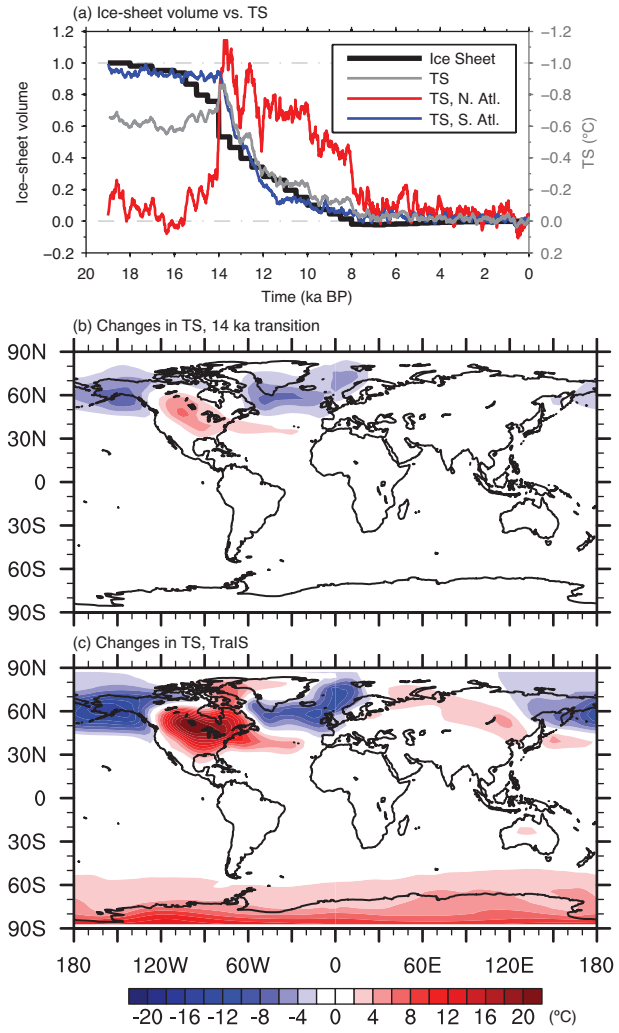

Figure S2.

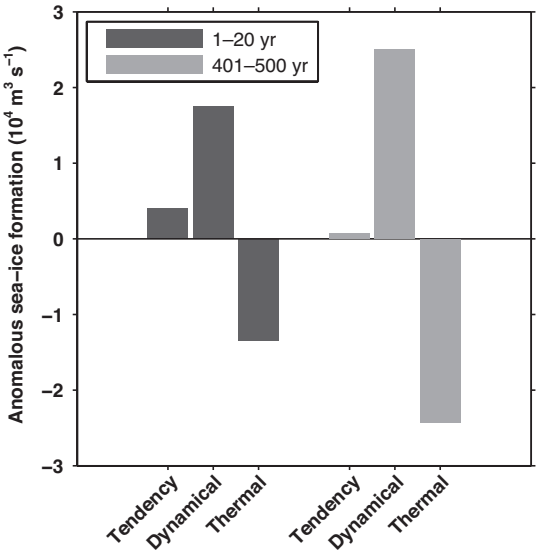
1–20 yr
401–500 yr
Anomalous sea–ice formation (10^4 m^3 s^{-1})
3
2
1
0
−1
−2
−3
Tendency
Dynamical
Thermal
Tendency
Dynamical
Thermal

Figure S3.

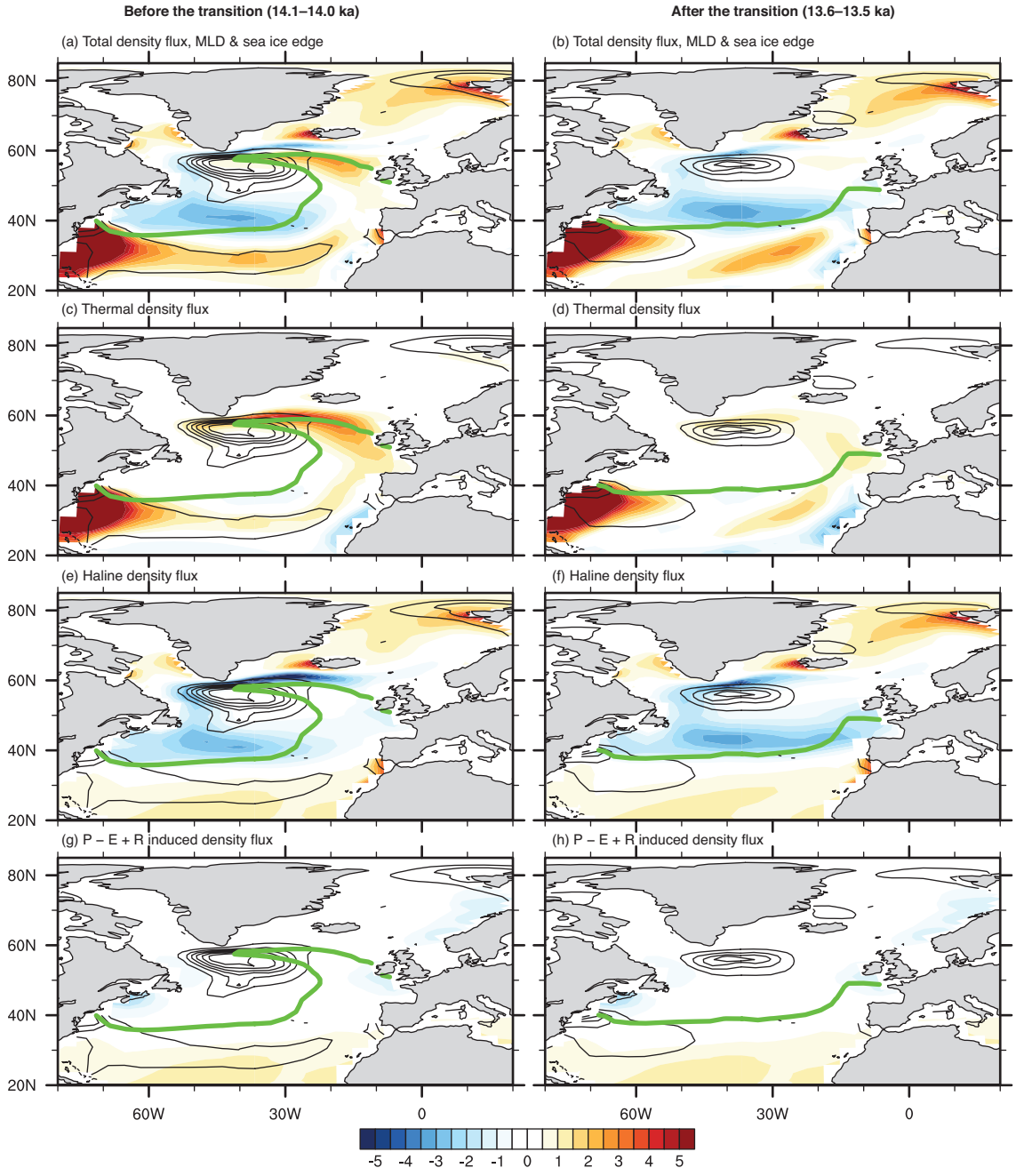
Before the transition (14.1–14.0 ka)
After the transition (13.6–13.5 ka)
(a) Total density flux, MLD & sea ice edge
(b) Total density flux, MLD & sea ice edge
(c) Thermal density flux
(d) Thermal density flux
(e) Haline density flux
(f) Haline density flux
(g) P – E + R induced density flux
(h) P – E + R induced density flux
80N
60N
40N
20N
60W
30W
0
-5 -4 -3 -2 -1 0 1 2 3 4 5

Figure S4.

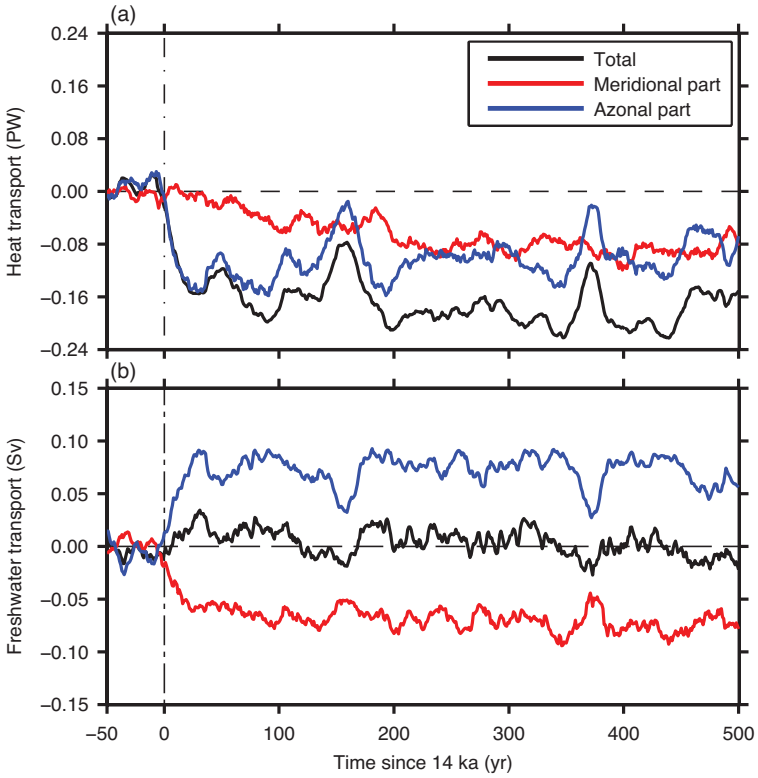
(a)
Total
Meridional part
Azonal part
Heat transport (PW)
0.24
0.16
0.08
0.00
−0.08
−0.16
−0.24
(b)
Freshwater transport (Sv)
0.15
0.10
0.05
0.00
−0.05
−0.10
−0.15
−50
0
100
200
300
400
500
Time since 14 ka (yr)

Text S1–S4

Text S1

In response to the deglacial ice-sheet retreat, the global mean surface temperature generally increases (Figure S1a) by a total value of about 0.6 ºC. Changes in surface temperature could be caused directly by the lowered topography and the decreased local albedo (both favoring a higher temperature), and indirectly by variations in other climate components, e.g., the atmosphere, ocean and sea ice. The simulated surface temperature increases approximately linearly after the 14 ka transition, which could be largely explained by the direct topography and albedo effect. However, it is interesting to note that, before 14 ka, especially during 17–14 ka, the global mean temperature decreases with the lowering of ice sheets, indicating significant indirect influence from other components. This decrease in temperature mainly comes from the Northern Hemisphere. We argue that the wind-driven expansion of sea ice is causing this (Figure 3). The fast and greatly expanding sea ice could insulate the ocean from heat loss to the atmosphere in northern high latitudes, leading to a cooler atmosphere above. Moreover, the cooling could be amplified by the sea ice-albedo positive feedback.

The temperature difference before and after the 14 ka transition could be as large as −5 ºC in the subpolar Atlantic and the northeastern Pacific Ocean including the Alaska region (Figure S1b), a magnitude comparable to major abrupt climate changes during the last deglaciation. We attribute this cooling mainly to the wind-driven sea ice expansion and the reduced northward heat transport by both the weakened subpolar gyre and the AMOC (Figure S3a). Therefore, it is

suggested that the topographic effects alone from a fast enough ice-sheet change could cause abrupt shifts in regional climate.

After the deglacial removal of ice sheets, the temperature response depicts a marked dipole mode—cooling in the north and warming in the south—except for the local warming over the North American continent and part of the Greenland and East Asia. The regional cooling over the subpolar regions and the GIN (Greenland, Icelandic, and Norwegian) Seas could reach −20 ºC. In addition to the direct effects from receding ice sheets, the warming in the south (and part of the cooling in the Northern Hemisphere) could be partly attributed to the reduced AMOC and northward heat transport.

Text S2

Our analysis demonstrates that the expansion of sea ice in the subpolar Atlantic (50ºN–70ºN) after the 14 ka transition is dominated by the dynamical sea-ice tendency (Figure S2), suggesting that the sea-ice expansion is caused mainly by anomalous transport, rather than local sea-ice formation. In the first several decades, the area-integrated dynamical sea-ice tendency in the subpolar Atlantic is about 1.7×10^4 m^3 s^{-1} and the thermodynamical sea-ice tendency is -1.5×10^4 m^3 s^{-1}. It suggests that there is a net sea-ice formation of 0.2×10^4 m^3 s^{-1} in the subpolar Atlantic, with dominating contribution from sea-ice transport. This is consistent with our wind-driven sea-ice expansion mechanism. Afterwards, the sea-ice increase from transport is only slightly larger than the sea-ice decrease from melting, leading to a very small net sea-ice forming.

Text S3

Figure S3 shows surface density fluxes in the North Atlantic before and after the 14 ka transition. Before 14 ka, the deep convection region, as represented by the average March mixed

layer depth (Figure S3a, black contour), lies to the south of Greenland right along the February sea-ice margin. The decomposition of the surface density flux suggests that the deep-water formation is primarily contributed by the positive thermal component (Figure S3c, warm shading) due to heat loss while the haline component makes negative contributions (Figure S3e, cool shading) due to freshwater flux from sea-ice melting (difference between Figure S3e and S3g). After the transition, in response to the fast wind-driven expansion of sea ice, the positive thermal density flux over the deep-water formation region weakens substantially (Figure S3d, warm shading), greatly reducing the total density flux (Figure S3b, warm shading) and the mixed layer depth (Figure S3b, black contour). Over the deep convection region, the haline density fluxes also change significantly (Figure S3f); however, they are caused mainly by the shift of the sea-ice margin and it contributes both positive and negative density fluxes such that the net impact on deep convection is limited (see also Figure 4a).

Text S4

Many feedbacks, including changes in the gyre systems, with various strength, could be involved to impact the response of the AMOC [*Born et al.*, 2010; *Swingedouw et al.*, 2007; *Timmermann and Goosse*, 2004]. Herein, we qualitatively analyze those associated with transport by ocean circulations. The transport across a certain latitude M_{T} can be separated into the meridional part (M_{MOC}) and the azonal part (M_{az}). Using the freshwater transport as an example,

$$M_{\mathrm{MOC}} = -\frac{1}{S_0}\int \bar{v}(z)\cdot(\langle\bar{S}\rangle - S_0)\cdot \mathrm{d}z \qquad \text{(S1)}$$

$$M_{\mathrm{az}} = -\frac{1}{S_0}\int \overline{v(z)'\cdot S'}\cdot \mathrm{d}z \qquad \text{(S2)}$$

where the reference salinity S_0 is the averaged salinity of the Atlantic Ocean (36.5 for the LGM). Here $\bar{v}(z)$ and $\langle\bar{S}\rangle$ denote the zonally integrated northward velocity and averaged salinity, and $v(z)'$ and S' represent the deviations from their zonal means.

The northward heat transport in the Atlantic Ocean across 45 ºN by both the AMOC and the subpolar gyre decreases significantly after the 14 ka transition (Figure S4a), with a total reduction of approximately −0.2 PW. The reduced northward heat transport favors a greater sea-ice formation and expansion, which could inhibit deep convection and weaken the AMOC further, forming the coupled sea ice-ocean positive feedback. It is worth noting that the reduction in gyre heat transport is faster and larger than the meridional part in the first 100–200 years, after which its magnitude is comparable with that of the AMOC.

Changes in the total freshwater transport are insignificant (−0.002 Sv), and, therefore are not important for the response of the AMOC (Figure S4b). However, this results from a cancelation between the gyre transport (0.07 Sv) and the AMOC transport (−0.07). The increased (decreased) freshwater (salt) transport by the weakened subpolar gyre could act as a positive feedback to amplify the reduction of the AMOC [*Born et al.*, 2010; *Timmermann and Goosse*, 2004]. In the meantime, the decreased (increased) freshwater (salt) transport by the AMOC could act as a negative feedback to stabilize the AMOC. The net effect is insignificant, because of the cancelation between the two.

References

Born, A., K. Nisancioglu, and P. Braconnot (2010), Sea ice induced changes in ocean circulation during the Eemian, *Climate Dynamics*, *35*(7-8), 1361-1371.

Swingedouw, D., P. Braconnot, P. Delecluse, E. Guilyardi, and O. Marti (2007), Quantifying the AMOC feedbacks during a 2×CO2 stabilization experiment with land-ice melting, *Climate Dynamics*, *29*(5), 521-534.

Timmermann, A., and H. Goosse (2004), Is the wind stress forcing essential for the meridional overturning circulation?, *Geophysical Research Letters*, *31*(4), L04303.